ACS APPLIED MATERIALS & INTERFACES

www.acsami.org

Research Article

Nb Texture Evolution and Interdiffusion in Nb/Si-Layered Systems

Anirudhan Chandrasekaran,* Robbert W.E. van de Kruijs, Jacobus M. Sturm, and Fred Bijkerk

Cite This: *ACS Appl. Mater. Interfaces* 2021, 13, 31260–31270

Read Online

ACCESS | Metrics & More | Article Recommendations

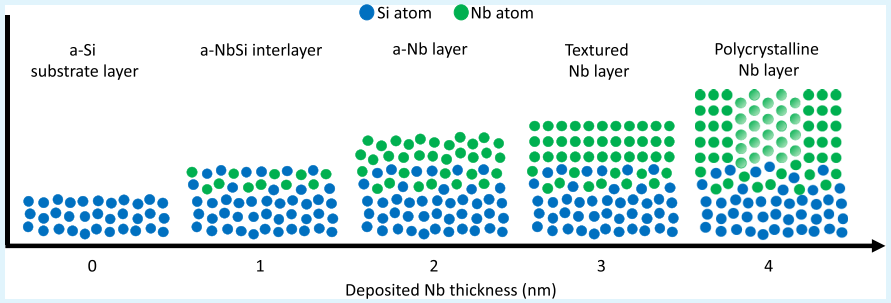

ABSTRACT: In this paper, we present a detailed study on the microstructure evolution and interdiffusion in Nb/Si-layered systems. Interlayer formation during the early stages of growth in sputter-deposited Nb-on-Si and Si-on-Nb bilayer systems is studied *in vacuo* using a high-sensitivity low-energy ion-scattering technique. An asymmetric intermixing behavior is observed, where the Si-on-Nb interface is ∼2× thinner than the Nb-on-Si interface, and it is explained by the surface-energy difference between Nb and Si. During Nb-on-Si growth, the crystallization of the Nb layer occurs around 2.1 nm as-deposited Nb thickness with a strong Nb(110)-preferred orientation, which is maintained up to 3.3 nm as-deposited Nb thickness. A further increase in the Nb layer thickness above 3.3 nm results in a polycrystalline microstructure with a reduced degree of texture. High-resolution cross-sectional transmission electron microscopy imaging is performed on Nb/Si multilayers to study the effect of the Nb layer texture on interdiffusion during low-temperature annealing. Nb/Si multilayers with amorphous 2 nm Nb layers and strongly textured 3 nm thick Nb layers, with limited grain-boundary pathways for diffusion, show no observable interdiffusion during annealing at 200 °C for 8 h, whereas in a Nb/Si multilayer with polycrystalline 4 nm thick Nb layers, a ∼1 nm amorphous Nb/Si interlayer is formed at the Si-on-Nb interface during annealing.

KEYWORDS: *metal−silicon interface, preferred orientation, interdiffusion, ion channeling, low-energy ion-scattering, thin film growth, sputter deposition*

1. INTRODUCTION

The extensive research work on transition-metal/silicon (TM/Si)-layered thin-film structures is generally motivated by their importance in several technological applications besides the interest in exploring the fundamental physics phenomena. The practical applicability of these structures in advanced technologies relies on, and more often is limited by, their interface quality and thermal stability. Both are inherently related to structural properties, such as the roughness, density, defects, grain size, and preferred orientation[1,2] of individual layers in the stack. For this reason, much efforts have been taken in the past decades to understand the influence of structural properties of constituting layers on the functional properties of thin-film devices.

Nb/Si-layered systems are widely used in superconductor applications.[3,4] Nb/Si-based multilayers have potential application in X-ray optics because of their favorable optical properties, thermal stability, and irradiation damage resistance.[5,6] Thin Nb layers can be used as a barrier in TM/Nb/Si and TM/Nb/SiO_2 systems,[7] which have useful applications in integrated circuits. The existing literature on Nb/Si multilayers unanimously report the asymmetry in interface width (Si-on-Nb interface is thinner than Nb-on-Si) for as-deposited structures, while the diffusion of Si and formation of the Nb_3Si phase at the interface are commonly observed during annealing.[8−11] Nevertheless, an understanding on the influence of structural properties of Nb layers on interdiffusion during annealing is still lacking. For instance, Okolo et al.[12] reported a strong (110) preferred orientation in Nb films that depends on Nb-layer thickness and the substrate material. However, to our knowledge, there are no studies in the literature that report the

Received: April 4, 2021
Accepted: June 10, 2021
Published: June 24, 2021

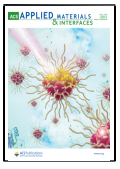

https://doi.org/10.1021/acsami.1c06210
ACS Appl. Mater. Interfaces 2021, 13, 31260−31270

effect of Nb layer texture on interdiffusion at Nb/Si interfaces. This knowledge can be beneficial in the fabrication of Nb layers with improved interface and barrier properties for Nb/Si-based thin-film systems.

The aim of this work is to study the microstructure evolution of the Nb layer in the first few nanometers during growth on a Si layer and investigate the influence of the Nb microstructural properties on the extent of interdiffusion at Nb/Si interfaces during annealing. The near-room-temperature layer growth and intermixing phenomena in Si-on-Nb and Nb-on-Si bilayer systems are studied using the *in vacuo* high-sensitivity low-energy ion-scattering (HS-LEIS) technique. Nb/Si multilayers with different Nb thicknesses are deposited to study the effect of Nb texture on thermal stability using high-resolution transmission electron microscopy (HR-TEM).

2. EXPERIMENT AND METHODOLOGY

Deposition and Characterization. All the samples were deposited using a direct-current magnetron sputtering technique on single side polished Si(100) wafers with ∼1 nm native oxide and 0.15 ± 0.05 nm root-mean-square (rms) roughness. A bilayer architecture, as shown in Figure 1, is used

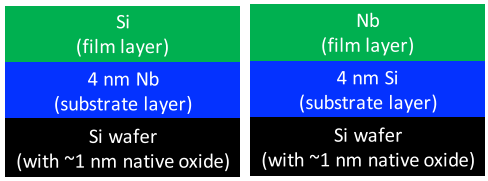

Figure 1. Bilayer architecture used for Si-on-Nb and Nb-on-Si layer growth studies.

for Si-on-Nb and Nb-on-Si LEIS layer growth studies. Bilayer samples for layer growth studies were deposited in a sputter deposition chamber with *in vacuo* sample transfer to a HS-LEIS setup. The base pressure of the deposition chamber and the Kr gas working pressure were $<5 \times 10^{-9}$ mbar and 1×10^{-3} mbar, respectively. Kr sputter gas was chosen instead of conventional Ar sputter gas in order to limit the number of high-energy backscattered neutrals bombarding the growing Nb film layer, which can induce intermixing at early stages of Nb-on-Si growth. The substrate-to-target distance was 8 cm for both materials. Both magnetrons were equipped with a shutter in front to prevent cross-contamination and a quartz crystal microbalance in close proximity to monitor the deposited thickness. The deposition rates of Nb and Si were calibrated using ex-situ grazing incidence X-ray reflectivity (GI-XRR) measurements on Nb and Si layers each with three different thicknesses, respectively, for better accuracy. The sputter power values used for Nb and Si were 25 and 18 W, respectively, and the corresponding sputter voltages were 320 and 540 V. A low-sputter power was chosen for both materials to get a low growth rate (Nb: 0.03 and Si: 0.05 nm/s), which is important to achieve a sub-nanometer (0.3 nm) growth step. The thickness accuracy of the deposited films is ±0.05 nm. The Nb/Si multilayer samples, with a 4 nm Si cap to prevent the oxidation of the stack, were produced in a Roth & Rau MS1600 deposition system under similar deposition conditions as compared to the depositions for *in vacuo* layer growth studies, such as sputter voltage, sputter gas, and pressure, and substrate-to-target distance. Hence, similar particle energies and layer microstructures can be expected during growth in both deposition systems.

The HS-LEIS technique was used to study the change in surface coverage as a function of the as-deposited film layer thickness in Nb-on-Si and Si-on-Nb systems. HS-LEIS measurements were performed using an IONTOF Qtac100 tool with 1×10^{-10} mbar base pressure. A 3 keV ion beam with 3 nA ion current and a 5 keV ion beam with 1 nA ion current at a normal incidence angle were used for He^+ and Ne^+ LEIS measurements, respectively. An Ar^+ sputter gun operating at 59° incidence angle relative to the surface normal with 0.5 keV ion energy and 100 nA ion current was used for sputter depth profile measurements. More information on the HS-LEIS technique can be found in refs 13 and 14.

The grazing incidence X-ray diffraction (GI-XRD) technique was used to investigate the crystalline properties of the multilayer samples. GI-XRD measurements were done using an in-house PANalytical Empyrean X-ray diffractometer with a Cu-Kα source (1.5406 Å). A BRUKER Dimension Edge atomic force microscope with a high-resolution tip (Mikro-Masch HiRes-C15/Cr−Au) was used for surface morphology characterization. The multilayer samples were annealed at 200 °C for 8 h in a high-vacuum environment to limit the oxidation of the layers. High-resolution cross-sectional transmission electron microscopy (XTEM) was used to study the structural and interface properties of as-deposited and annealed multilayer samples. XTEM images were obtained using a Philips CM300ST-FEG transmission electron microscope (300 kV acceleration voltage) at the MESA + Institute, University of Twente. The specimens for XTEM were prepared by creating a symmetrical cross-sectional sandwich structure using dimple grinding/polishing and argon ion thinning methods.[15,16] In the final stages of Ar^+ thinning, the energy of Ar^+ was reduced from 4.5 to 0.5 keV to minimize specimen damage.

LEIS Growth Profile. Thin-film interfaces are usually studied using techniques such as X-ray photoelectron spectroscopy (XPS), XRR, and XTEM. Using these techniques, it is possible to obtain the interface concentration profile and the effective interface width by considering a suitable thin-film model that fits the experimental data well.[17−20] The significance of the HS-LEIS technique is its high surface sensitivity, which when coupled with the *in vacuo* sample-transfer facility allows us to measure the evolution of surface coverage during layer growth ("growth profile").[21,22] This provides key information about the film layer closing thickness, surface atomic densities, surface segregation, and other surface phenomena during growth that cannot be studied using conventional techniques. In addition, the interface profile and the effective interface width can also be extracted from LEIS growth profiles by considering an appropriate interface model.[21−23] The following procedure was used to record LEIS spectra for the layer growth studies:

(1) A 4 nm substrate layer was deposited onto a Si wafer, followed by a 0.3 nm film layer.
(2) The sample was transferred *in vacuo* to the LEIS chamber and a LEIS spectrum was recorded.
(3) A 4 nm substrate layer was deposited onto a new Si wafer, followed by the film layer with a sub-nanometer increase in thickness.
(4) Steps 2 and 3 were repeated until the film layer signal during LEIS measurements saturates, which corresponds to a 100% film coverage.

https://doi.org/10.1021/acsami.1c06210
ACS Appl. Mater. Interfaces 2021, 13, 31260−31270

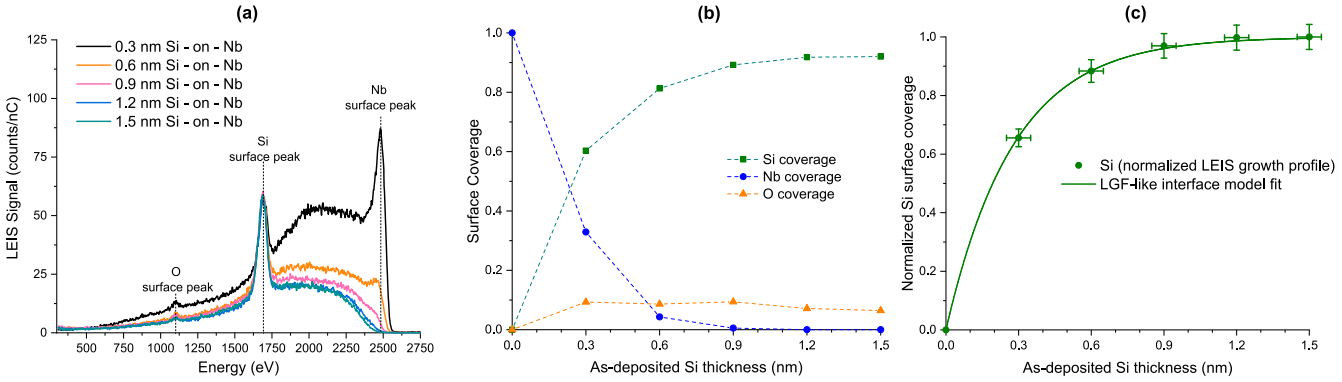

Figure 2. (a) He^+ LEIS spectra of Si-on-Nb growth for various as-deposited Si thicknesses, (b) LEIS growth profiles of Si, Nb, and O as a function of as-deposited Si thickness, and (c) normalized Si LEIS growth profile with an LGF-like interface model fit.

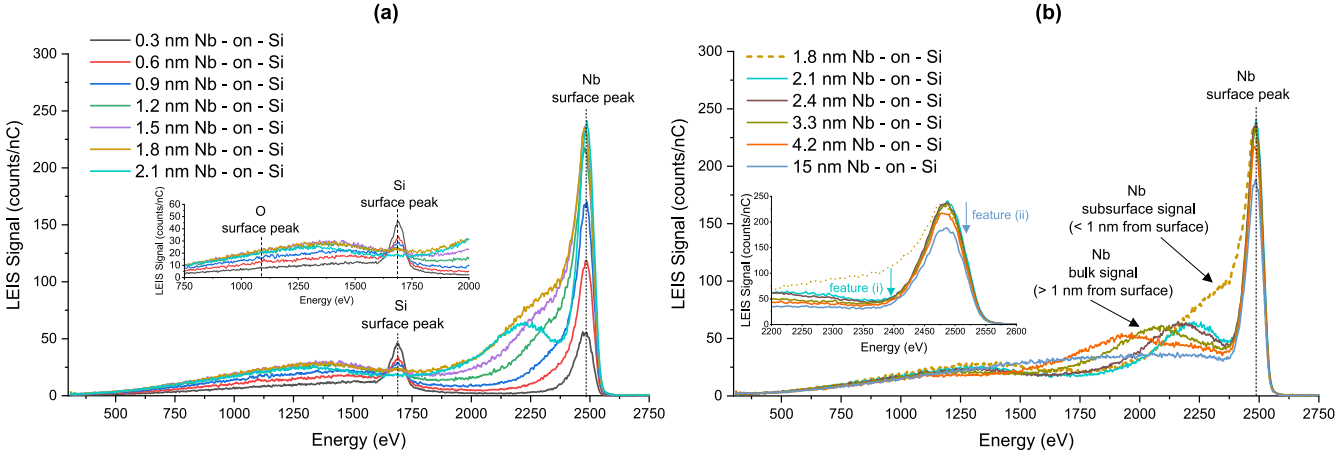

Figure 3. He^+ LEIS spectra of Nb-on-Si growth split into two figures for better visibility: (a) 0.3 to 2.1 nm as-deposited Nb thickness and (b) 1.8 to 15 nm as-deposited Nb.

A quantitative measurement of the number of surface atoms of a certain element can be obtained from the integral of the corresponding LEIS surface peak after subtracting the background signal. The surface coverage of an element is given by the ratio of the integral of the surface peak in the investigated sample to that of a clean reference sample. Because LEIS cannot distinguish between intermixing and island formation processes during growth, *ex-situ* AFM measurements were done to characterize the surface morphology of the deposited layers.

It has been recently shown that the interface profile between two layers caused by intermixing during deposition near room temperature can be mathematically represented by a logistic function (LGF) of the form[22,23]

$$C(z) = \frac{1}{1 + e^{(z - z_i/0.59\sigma)}} \quad (1)$$

where C is the concentration of the deposited film atom at a depth z from the surface, z_i is the point of inflection of the logistic function, and σ is the effective width of the interface. Based on an LGF-like interface model, the expression for the evolution of the film atom surface coverage θ as a function of the as-deposited film layer thickness h can be derived as

$$\theta = 1 - e^{-\left(\frac{h}{0.59\sigma}\right)} \quad (2)$$

The effective interface width of Si-on-Nb and Nb-on-Si systems can be obtained by fitting their respective LEIS growth profiles using eq 2, which is comparable to the interface width obtained from XRR spectra assuming an error function-like interface model.

3. RESULTS AND DISCUSSION

LEIS Layer Growth Studies: Si-on-Nb and Nb-on-Si Bilayer Systems. The He^+ LEIS spectra of the Si-on-Nb system for various Si thicknesses are shown in Figure 2a. The He primary ions that scatter from surface atoms contribute to the surface peaks, whereas ions that scatter from the subsurface atoms (up to ~10 nm depth) contribute to the low-energy tail. Besides surface peaks of Nb and Si atoms, there is a small contribution from impurity O atoms at the surface, which may arise from the presence of background residual oxygen and water during *in vacuo* sample transfer (~7 min transfer time at 1×10^{-9} mbar). AFM images (not shown here) of 0.3 nm and 0.9 nm Si-on-Nb indicate a typical 2D growth with rms surface roughness in the range of ~0.2 ± 0.05 nm. This means that the change in the surface peak intensity with increasing as-deposited Si thickness is an effect of intermixing during film layer growth and not because of a change in surface morphology.

The surface coverage evolution of Nb, Si, and O atoms as a function of as-deposited Si thickness is shown in Figure 2b. The reference surface peak integral values for Nb and Si are obtained from their clean reference samples. The reference value for O (1180 counts/nC) is taken from the work of

https://doi.org/10.1021/acsami.1c06210
ACS Appl. Mater. Interfaces 2021, 13, 31260−31270

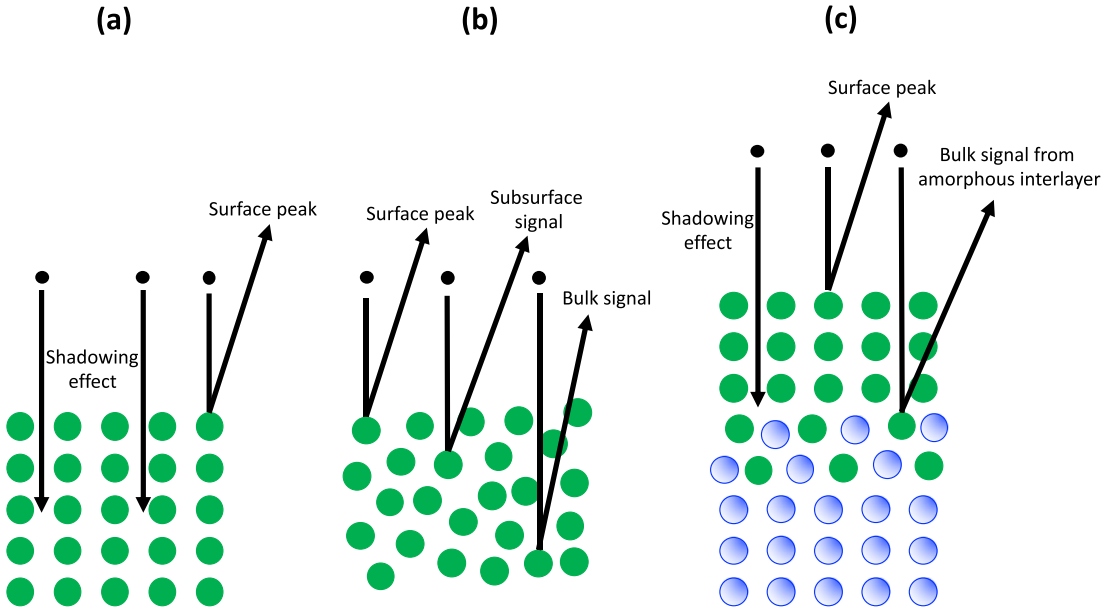

Figure 4. Schematic representation of LEIS from: (a) a crystalline layer, (b) an amorphous layer, and (c) a crystalline film layer with an amorphous interlayer at the interface between the film layer and the substrate layer.

Coloma Ribera et al.[21] The surface coverage of Si atoms does not reach 100% even when the Nb surface coverage goes to 0% because of the presence of O atoms at the surface. Because the surface coverage of O is constant for all samples, we use the normalized Si surface coverage values to obtain the effective interface width. The normalized Si LEIS growth profile with an LGF-like interface model fit (eq 2) is shown in Figure 2c. The fit based on an LGF-like interface model describes the experimental data well, and the effective width of the Si-on-Nb interface obtained from the LEIS growth profile fit is 0.47 ± 0.03 nm. The effective interface width obtained from the LEIS growth profile is analogous to the interface width usually obtained from the XTEM and XRR techniques. The as-deposited Si thickness required to obtain a 99% Si surface coverage ("intermixing thickness") is calculated from the LEIS fit as 1.3 ± 0.1 nm.

A similar approach is taken to study the layer growth of Nb-on-Si. The He^+ LEIS spectra of the Nb-on-Si system for various Nb thicknesses are shown in Figure 3. AFM images (not shown here) show a typical 2D growth with rms surface roughness in the range of 0.2 ± 0.05 nm, again indicating that the observed changes in LEIS spectra are because of intermixing and not surface morphology. The Nb-on-Si LEIS spectra show two peculiar features, as indicated in Figure 3b: (i) at 2.1 nm as-deposited Nb thickness, the intensity of the low-energy Nb tail close to the Nb surface peak drops significantly and (ii) reduction in the Nb surface peak intensity after 3.3 nm as-deposited Nb thickness.

To understand the drop in intensity near the surface peak at 2.1 nm Nb [feature (i)], it is important to look in more detail to the origin of the low-energy Nb tail in the LEIS spectra.[13,24] The 3 keV He primary ions are neutralized once they enter the surface layer because of high neutralization probability. The neutral He atoms that backscatter from sub-surface Nb atoms have to be reionized at the surface level in order to be detected. Therefore, the shape and intensity of the low-energy Nb tail depends both on the number of He neutrals backscattered from the Nb atoms distributed in depth, and the probability of reionization of these neutrals at the surface level. The reionization probability is material specific and is influenced by the surface composition.[13,24] However, a small change in the surface composition from 1.8 to 2.1 nm of Nb-on-Si alone cannot explain the observed changes in the slope and intensity of the low-energy tail near the surface peak. The absence of other surface peaks except Nb eliminates the role of surface contamination, while surface roughness can be excluded because of low rms roughness values obtained from AFM images. Hence, the change in the low-energy tail is not because of surface effects but has to be caused by sub-surface effects. The number of He neutrals backscattered from the bulk depends on the in-depth Nb concentration. A decrease in the Nb concentration in the sub-surface layers would result in a reduced tail intensity close to the Nb surface peak. However, the possibility of Nb atoms being physically absent in the sub-surface layers is highly unlikely because of the negligible bulk diffusion near room temperature.

Another possible reason for a drop in the low-energy tail intensity close to the surface peak is the "shadowing" of sub-surface atoms by surface atoms, as shown in Figure 4a, which leads to the channeling of He neutrals through sub-surface layers into bulk layers without backscattering. This effect is normally observed in single-crystalline layers under a specific geometry, and it results in a strong reduction in the backscattering contribution from the sub-surface layers.[25,26] During the growth of the metal on Si layers in metal/Si multilayers, an abrupt crystallization of the metal layer is usually observed around an as-deposited metal thickness of 2−3 nm, resulting in typically 1 nm of the crystalline metal layer on top of an amorphous metal-Si intermixed zone.[27] In order to verify the Nb crystallization step around 2.1 nm, a LEIS sputter profile measurement was performed on a Nb-on-Si sample after the crystallization step. The 500 eV Ar^+ sputtering is expected to result in the amorphization of the crystalline Nb layer, which should eliminate the channeling effect (Figure 4b) and thereby, increase the backscattering contributions from the sub-surface Nb atoms to the precrystallization level. Figure 5 shows the LEIS sputter depth profile measurement of a 2.4 nm Nb-on-Si sample, in which the expected increase in the

https://doi.org/10.1021/acsami.1c06210
ACS Appl. Mater. Interfaces 2021, 13, 31260−31270

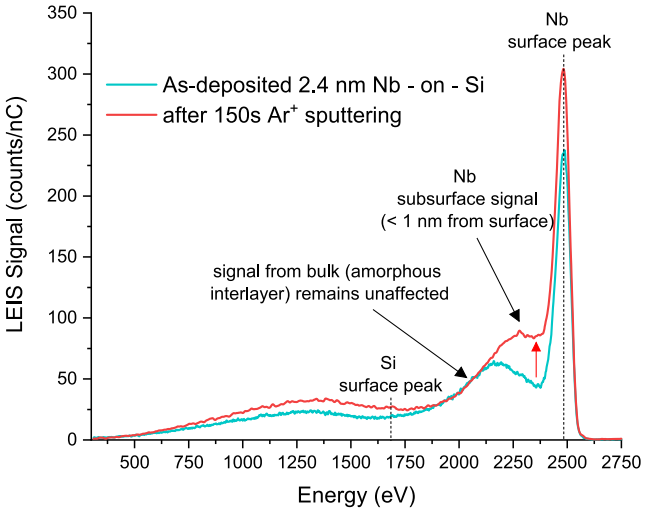

Figure 5. He^+ LEIS spectra of 2.4 nm Nb-on-Si: as-deposited and after 500 eV Ar^+ sputtering for 150 s.

intensity of the low-energy tail just below the surface peak can be seen after Ar^+ sputtering. The tail contribution from deeper amorphous Nb−Si intermixed layers remains unaffected. The elimination of the channeling effect by sputter ion-induced amorphization confirms the crystallization of Nb around 2.1 nm as-deposited thickness. Note that the increase in the Nb surface peak signal after sputtering is because of the removal of residual H and OH at the surface.

A Nb crystallization step around 2.1 nm is a reasonable explanation for the drop only in the subsurface Nb tail contribution (crystalline part), while the contribution from the deeper amorphous intermixed zone remains unaffected (Figure 4c). However, it is important to note that sputter-deposited metals usually form a polycrystalline structure after crystallization, in which the channeling effect is expected to be insignificant. Therefore, a highly textured (preferred orientation) Nb layer must be formed after crystallization for channeling to occur. The most densely packed (hkl) plane is generally preferred during the layer growth because of the low surface energy. For bcc metals, the densely packed (110) plane has the lowest surface energy when compared to other (hkl) planes[28] and, therefore, it is likely that bcc Nb layers show a (110) preferred orientation during Nb-on-Si growth. A strong texture in sputter-deposited Nb layers with a (110) preferred orientation has also been reported before.[11,12] We will later show the GI-XRD results of Nb/Si multilayers studied in this work, which confirm the Nb(110)-preferred orientation after crystallization. Based on these pieces of evidence, it is possible to conclude that a strongly textured Nb layer is formed after the crystallization step around 2.1 nm during the growth of Nb-on-Si.

The feature (ii) observed in the Nb-on-Si LEIS spectra (Figure 3b) is the reduction in the Nb surface peak intensity for Nb thicknesses above 3.3 nm. The complex shape of the tail in the case of Nb-on-Si LEIS spectra makes it difficult to subtract the background for the calculation of the Nb surface peak integral. In order to overcome this problem, we use Ne^+ for LEIS measurements on newly prepared Nb-on-Si samples, for which the intensity of the low-energy tail is considerably lower than in He^+ measurements and, therefore, its impact on the surface peak is negligible. The Ne^+ LEIS spectra of Nb-on-Si growth are shown in Figure 6a,b, and the surface peak integral value for each Nb thickness is shown in Figure 6c. The Nb surface peak integral value increases up to around 2.1 nm Nb and then starts to decrease from 3.3 nm Nb up to 6 nm Nb, after which it saturates around 53,000 counts/nC. As the surface peak integral is a direct measure of the number of surface atoms, a decrease in the integral value implies a decrease in the number of Nb surface atoms. In the absence of other elements at the surface, the decrease in the Nb surface signal can be caused by a reduction in density as a result of a porous growth, or by a significant change in Nb crystal orientations, resulting in a net change in the surface atomic density. A porous layer with ∼15% lower density than the bulk layer is required to explain the observed decrease in the surface peak integral. Low-pressure magnetron sputtering deposition generally produces high density films and hence, a porous layer growth is highly unlikely. Thus, the reduction in the surface peak integral between 3.3 and 6 nm as-deposited Nb thicknesses suggests a change in surface atomic density due to the structural evolution of the Nb layer. The observed LEIS growth profile can be explained by a textured Nb growth with high surface density planes up to 3.3 nm, followed by a polycrystalline growth with a reduced average surface atomic density up to 6 nm. We will later show the GI-XRD and XTEM results of Nb/Si multilayers that support this explanation.

It is important to note that the surface peak integral reaches a value of ∼53000 counts/nC (similar to 6 nm and 15 nm Nb) already at 1.5 nm Nb even in the presence of ∼8% Si surface coverage, which indicates a preference toward high surface atomic density even before the crystallization step. This suggests that the tendency to form a high surface density structure is most likely influenced by the Si substrate atoms. In our previous work,[22] we showed the importance of surface energy and strain energy on intermixing and segregation processes during growth. The low surface energy of Si facilitates the diffusion of Si to the surface during Nb-on-Si growth. However, the strain induced by a large size difference between Nb and Si (∼0.28 Å) facilitates the surface segregation of the large atom,[22] Nb in this case. The need to compete against the low surface energy Si in order to limit the Nb−Si intermixing, which would lead to a large strain energy, stimulates the textured growth of the Nb layer with a high surface density (110) preferred orientation (i.e., the lowest possible Nb layer surface energy). Further increase in Nb thickness leads to a polycrystalline growth with other low surface density planes in addition to the high surface density (110) plane. Okolo et al.[12] showed a greater degree of Nb texture on an amorphous Si_3N_4 substrate when compared to an amorphous SiO_2 substrate. The authors explain this based on the difference in the chemical interaction between Nb−O and Nb−N. However, we believe this is because of a stronger intermixing between Nb and Si during Nb-on-Si_3N_4 growth when compared to SiO_2, which facilitates a greater degree of textured growth on Si_3N_4. Coloma Ribera et al.[21] showed that the intermixing length decreases in the order of Ru-on-Si > Ru-on-Si_3N_4 > Ru-on-SiO_2. Therefore, assuming a similar growth for Nb on Si, Si_3N_4, and SiO_2, the Nb texture is expected to be stronger on Si > Si_3N_4 > SiO_2 substrate layers. Furthermore, Okolo et al.[12] showed an increased Nb-layer texture for sputter-cleaned substrates when compared to uncleaned substrates. The intermixing between Nb and Si (from Si_3N_4 and SiO_2 substrate layers) can be expected to be greater in the absence of surface contamination. This leads to an increased

https://doi.org/10.1021/acsami.1c06210
ACS Appl. Mater. Interfaces 2021, 13, 31260−31270

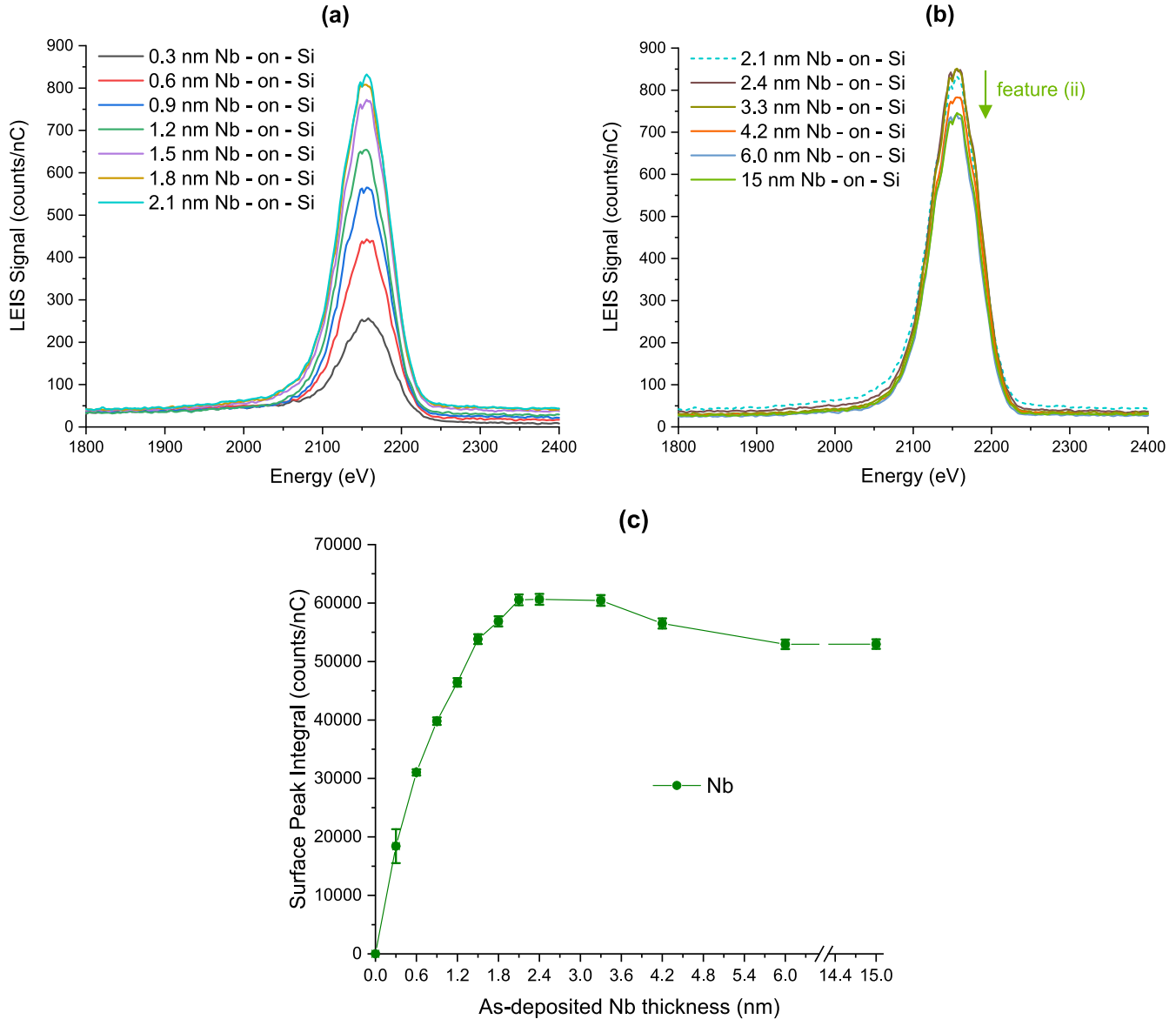

Figure 6. Ne^+ LEIS spectra of Nb-on-Si growth split into two figures for better visibility: (a) 0.3 to 2.1 nm as-deposited Nb thickness, (b) 2.1 to 15 nm as-deposited Nb thickness, and (c) Nb surface peak integral as a function of the as-deposited Nb thickness.

degree of Nb texture for cleaned substrates when compared to uncleaned substrates.

Because of Nb structural evolution up to 6 nm as-deposited thickness, it is not possible to consider a suitable Nb surface peak integral reference for the surface coverage calculation. The accuracy of the Nb reference surface peak integral is critical for the Nb surface coverage calculation which, in turn, determines the value of the effective interface width obtained from the growth profile fit. The complexity in the Nb layer surface evolution because of strong structural changes makes the LEIS growth profile fit based on a simple LGF-like interface model unreliable. For this reason, it is not possible to obtain an accurate value for the Nb-on-Si effective interface width from LEIS results. Nevertheless, comparing the normalized surface peak integral of Nb-on-Si and Si-on-Nb (Figure 7), it is possible to claim that the intermixing thickness of the Nb-on-Si interface is ~2 times that of Si-on-Nb. This means that the effective interface width of Nb-on-Si can be expected to be ~1 nm, which is confirmed by the XTEM results shown in the next section. This asymmetry in interface thicknesses has been reported before for Nb/Si systems,[11] other TM/Si systems,[21,29−31] and also for TM-on-TM systems.[22] The reason for the asymmetry is mainly because of the surface energy difference between Nb (1.85 eV/atom) and Si (0.92 eV/atom).[22,32] The low surface energy Si tends to move to the surface during growth to reduce the net surface free energy of the system. This leads to an increased intermixing during Nb-on-Si growth when compared to Si-on-Nb growth, where low energy Si is the film layer.

Interface Diffusion Studies: As-Deposited and Annealed Nb/Si Multilayer. The Nb-on-Si LEIS growth studies suggest the crystallization of the Nb layer around 2.1 nm as-deposited thickness, followed by a textured growth with high surface density planes up to 3.3 nm Nb thickness, and a polycrystalline growth with reducing average surface atomic density from 3.3 to 6 nm. The structural properties of the Nb layer can influence the diffusion of atoms through interfaces at high temperatures. In order to study the effects of the Nb

https://doi.org/10.1021/acsami.1c06210
ACS Appl. Mater. Interfaces 2021, 13, 31260−31270

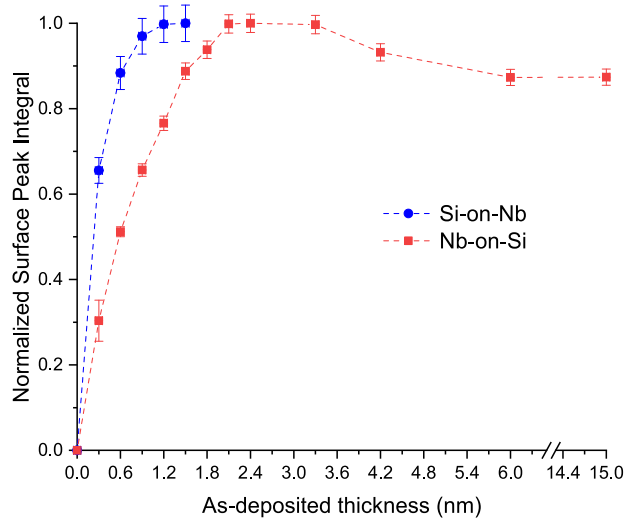

Figure 7. Normalized He^+ LEIS surface peak integral of the Si-on-Nb system and normalized Ne^+ LEIS surface peak integral of the Nb-on-Si system.

structure on interdiffusion during annealing, three different Nb/Si multilayers with 4 nm Si layers and Nb thicknesses of 2, 3, and 4 nm were deposited, which, from now on, will be referred to as Nb-2, Nb-3, and Nb-4 multilayers, respectively. As the intention of this study is to measure the interdiffusion at the interfaces without destroying the overall multilayer structure, Nb/Si multilayers were annealed at 200 °C for 8 h, for which interdiffusion effects are expected to be visible without significant structural modifications.[11]

The GI-XRD results of as-deposited Nb/Si multilayers are shown in Figure 8a. The higher order diffraction peaks are strongly suppressed in the Nb-2 multilayer, which suggests that the 2 nm Nb layers are quasi-amorphous or nanocrystalline with a short-range order. The broad peak around 38° is due to collective scattering from the nearest neighbors in the Nb layer. The GI-XRD spectra of Nb-3 and Nb-4 multilayers indicate a polycrystalline bcc Nb structure. The intensities of the diffraction peaks from a polycrystalline sample are expected to scale with the grain size and the thickness of the diffracting layer. However, in the case of the Nb-3 multilayer, the intensity of the (110) peak is lower than that of the Nb-2 multilayer, whereas other diffraction peaks are dominant. An incidence angle (ω) scan with a diffraction angle (2θ) fixed at 38° (Figure 8b) shows a steep increase in intensity around $\omega = 1/2\ 2\theta$, whereas the ω scans of other diffraction peaks with 2θ fixed at their respective diffraction angles (not shown here) show an exponential drop in intensity with increasing ω. This implies a strong Nb(110) preferred orientation parallel to the surface in the Nb-3 multilayer. The ω scan of the Nb-4 multilayer shows a reduced degree of the Nb(110)-preferred orientation when compared to the Nb-3 sample. This reduction in the degree of the preferred orientation of the highest density (110) planes between 3 and 4 nm Nb layers (i.e., a polycrystalline growth) is in accordance with the reduction in the Nb surface peak integral observed in the LEIS data (Figure 6c).

High-resolution cross-sectional transmission electron microscopy (XTEM) images were used to study the layer and interface changes in the multilayers after annealing. XTEM images of as-deposited and annealed Nb/Si multilayers are shown in Figure 9. The Si layers are amorphous in all as-deposited and annealed multilayer samples, whereas the Nb layers are quasi-amorphous in the Nb-2 multilayer and crystalline in Nb-3 and Nb-4 multilayers. The magnified regions in the Nb layers are shown to enhance the visibility of the Nb layer structure. The 3 nm Nb layers show a strong preferred orientation with planes predominantly parallel to the surface, whereas other orientations in addition to the planes parallel to the surface can be seen in the 4 nm Nb layers. The structure of Nb layers did not change after annealing in all three multilayers, as expected for a lower temperature annealing at 200 °C.

In the Nb-2 multilayer, the interfaces between the Nb and Si layers cannot be accurately resolved due to the low contrast between quasi a-Nb and a-Si layers. Nevertheless, the shape of the line profiles (shown in inset) of the as-deposited and annealed structures is identical, which suggests negligible interdiffusion at the interfaces as a result of annealing. In the as-deposited Nb-3 multilayer, a ~1.3 nm thick amorphous Nb-

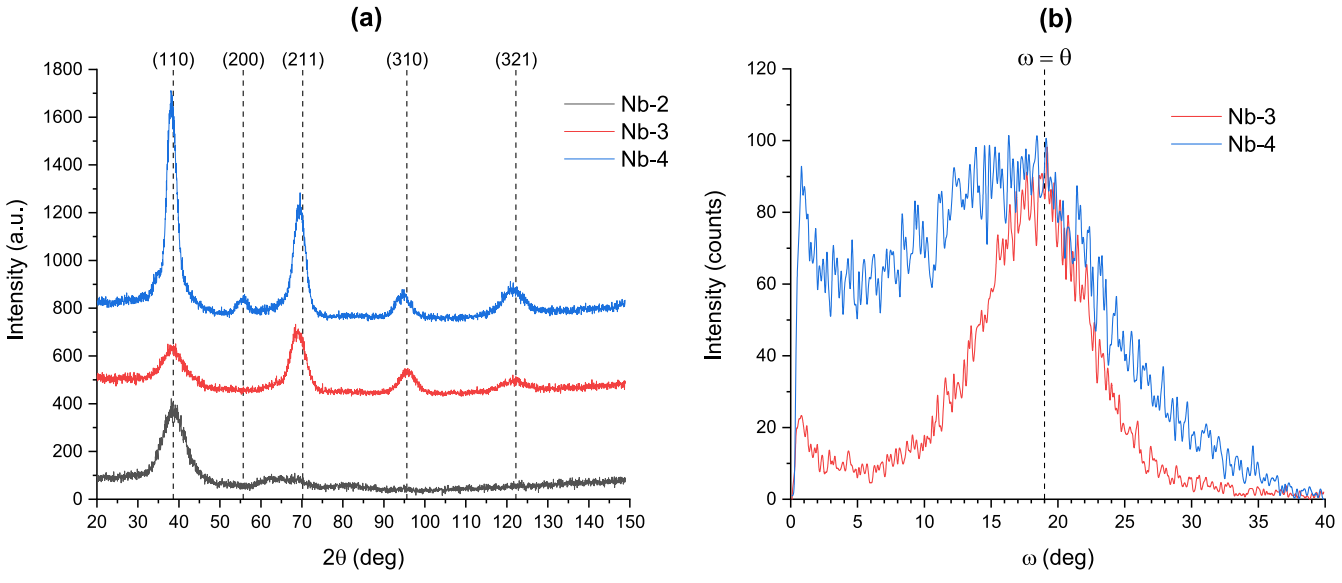

Figure 8. (a) GI-XRD spectra of Nb/Si multilayers and (b) incident angle [ω] scan with 2θ at 38° of Nb-3 and Nb-4 multilayers.

https://doi.org/10.1021/acsami.1c06210
ACS Appl. Mater. Interfaces 2021, 13, 31260−31270

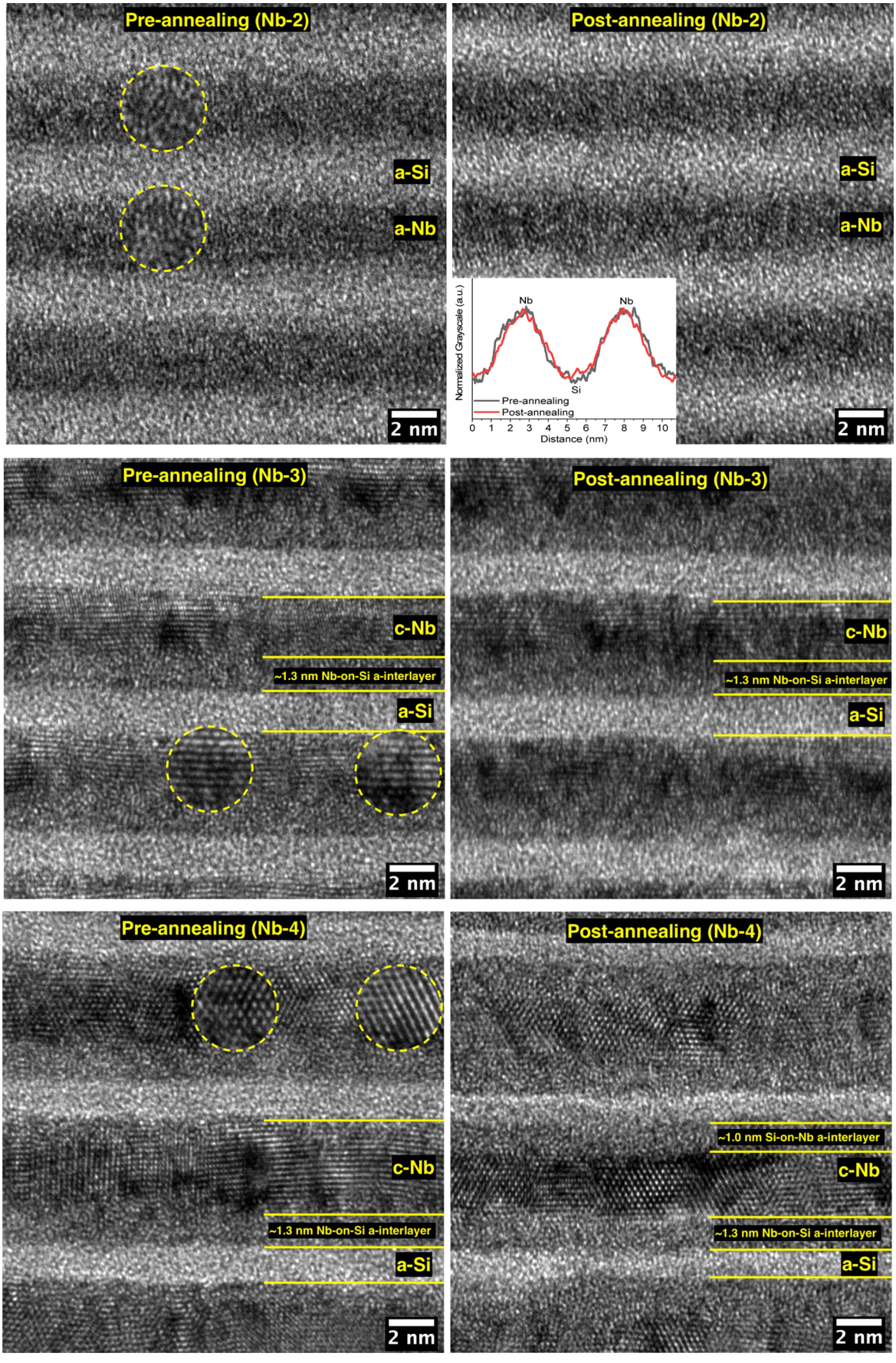

Figure 9. XTEM images of Nb/Si multilayers pre- and postannealing.

https://doi.org/10.1021/acsami.1c06210
ACS Appl. Mater. Interfaces 2021, 13, 31260−31270

on-Si interface can be seen. The polycrystalline Nb layers extend all the way up to the following (top) Si layer, indicating a sharp Si-on-Nb interface. Because of the negligible solubility of Si and Nb in each other at 200 °C,[33,34] interdiffusion between Nb and Si during annealing in general will lead to the solid-state amorphization of the polycrystalline Nb layer and formation of an intermixed Nb−Si amorphous interlayer. As the Nb layer and both interfaces remain unchanged within the resolution of the XTEM after annealing, it is possible to conclude that a significant interdiffusion did not occur during annealing at 200 °C in the Nb-3 multilayer sample. The Nb-on-Si and Si-on-Nb interfaces in the as-deposited Nb-4 multilayer are similar to that of the as-deposited Nb-3 multilayer. However, after annealing, although the Nb-on-Si interface remains unaltered similar to the case of the Nb-3 multilayer, the formation of a ∼1 nm thick amorphous interlayer at the Si-on-Nb interface can be clearly seen. This suggests a strong interdiffusion at the Si-on-Nb interface during annealing at 200 °C. The thickness reduction after annealing in the polycrystalline Nb and the amorphous Si layers is ∼1 and ∼0.5 nm, respectively, indicating that the amorphous interlayer formed at the Si-on-Nb interface is mostly Nb rich. This is also in accordance with previous studies,[8−11] which show the formation of a Nb_3Si phase above 300 °C.

The interdiffusion of layer materials during low-temperature annealing (100−250 °C) is a commonly observed phenomenon in metal/silicon systems.[35,36] At these temperatures, grain-boundary diffusion is generally more dominant when compared to vacancy diffusion through the bulk. Therefore, interdiffusion in the Nb-4 multilayer during annealing at 200 °C can be explained by the thermally activated diffusion of Si atoms into the Nb layer, which is enhanced by the presence of grain boundaries in the polycrystalline Nb layer. Although Nb layers in the Nb-3 multilayer are also polycrystalline, they are strongly textured when compared to Nb layers in the Nb-4 multilayer. This results in a reduced number of grain boundaries, and thereby restricts the available pathways for Si diffusion.[1] In the case of the Nb-2 multilayer, the absence of grain boundaries because of the quasi-amorphous nature of the Nb layers and the presence of trap (defect) sites can strongly limit interdiffusion. Hence, Nb-2 and Nb-3 multilayers show greater thermal stability at 200 °C when compared to the Nb-4 multilayer. Note that the Nb-on-Si interface remains unaffected in all three samples. This can be because of the presence of the ∼1.3 nm thick amorphous Nb−Si interlayer formed during growth that can act as a barrier in preventing further interdiffusion through that interface in all three multilayer samples.

Finally, it is important to realize that thermally activated interdiffusion in nanoscale thin-film structures initiates several distinct temperature-dependent processes, such as solid-state amorphization, phase formation, and crystallization. In this work, we have taken the first step in understanding the structural evolution of Nb layers during Nb-on-Si growth, and its importance on interdiffusion during low-temperature annealing. Further work is required to understand the effect of the Nb layer texture on complex physical processes activated at higher temperatures.

4. SUMMARY AND CONCLUSIONS

LEIS growth profiles were used to study intermixing phenomena during the early stages of growth in sputter-deposited Nb-on-Si and Si-on-Nb systems. A decrease in the Nb LEIS tail and surface peak intensities was observed during Nb-on-Si growth, which was attributed to crystallization and microstructure evolution of the Nb layer during growth. GI-XRD and XTEM studies were performed on Nb/Si multilayers, with different Nb thicknesses, to confirm the microstructure evolution of the Nb layer and investigate the effect of the Nb layer texture on interdiffusion during low-temperature annealing at 200 °C.

The following conclusions are derived:

- The as-deposited Si-on-Nb interface width is 0.47 ± 0.03 nm, which is approximately twice as sharp as the Nb-on-Si interface. The asymmetry in interface width is explained by the difference in surface energy between Si and Nb atoms. The low-surface energy Si atoms tend to move toward the surface during growth, resulting in a wider intermixing zone during Nb-on-Si growth when compared to Si-on-Nb growth.
- During Nb-on-Si growth, Nb crystallizes around 2.1 nm as-deposited thickness with a strong Nb(110)-preferred orientation. The large size difference between Nb and Si atoms can increase the strain energy at the Nb-on-Si intermixed zone, which is expected to stimulate the low surface energy Nb(110)-preferred orientation during the crystallization of the Nb layer. The textured growth continues up to 3.3 nm as-deposited Nb thickness, and further increase in Nb thickness results in a polycrystalline microstructure with a reduced degree of texture.
- Nb/Si multilayers with amorphous 2 nm Nb layers and strongly textured 3 nm Nb layers show no noticeable changes in the structure during low-temperature annealing at 200 °C because of the absence or limited number of grain-boundary pathways for the diffusion of Si atoms. In the Nb/Si multilayer with 4 nm polycrystalline Nb layers, diffusion occurs via grain boundaries resulting in a ∼1 nm amorphous interlayer at the Si-on-Nb interface. The Nb-on-Si interface remains unaltered because of the presence of a ∼1.3 nm amorphous interlayer that was formed during growth, which acts as a barrier layer in preventing further diffusion through that interface during low-temperature annealing.

As an overall conclusion, microstructural properties of metal layers in metal-Si thin-film systems play a crucial role in determining thermal stability in the low-temperature regime (up to ∼300 °C), where grain-boundary diffusion is expected to be the most dominant mechanism. Limiting grain-boundary pathways by stimulating textured growth or preventing the crystallization of thin metal layers may provide the possibility to improve the thermal stability and the device performance.

AUTHOR INFORMATION

Corresponding Author

Anirudhan Chandrasekaran − *Industrial Focus Group XUV Optics, MESA+ Institute for Nanotechnology, University of Twente, Enschede 7500 AE Enschede, The Netherlands;* orcid.org/0000-0003-3763-1423; Email: a.chandrasekaran@utwente.nl

Authors

Robbert W.E. van de Kruijs − *Industrial Focus Group XUV Optics, MESA+ Institute for Nanotechnology, University of Twente, Enschede 7500 AE Enschede, The Netherlands*

https://doi.org/10.1021/acsami.1c06210
ACS Appl. Mater. Interfaces 2021, 13, 31260−31270

Jacobus M. Sturm − *Industrial Focus Group XUV Optics, MESA+ Institute for Nanotechnology, University of Twente, Enschede 7500 AE Enschede, The Netherlands*

Fred Bijkerk − *Industrial Focus Group XUV Optics, MESA+ Institute for Nanotechnology, University of Twente, Enschede 7500 AE Enschede, The Netherlands*

Complete contact information is available at: https://pubs.acs.org/10.1021/acsami.1c06210

Notes

The authors declare no competing financial interest.

■ ACKNOWLEDGMENTS

This work was carried out at the Industrial Focus Group XUV Optics, MESA + Institute for Nanotechnology, University of Twente. We acknowledge the support and funding from the industrial partners ASML, Carl Zeiss GmbH, Malvern Panalytical, TNO, as well as from the Province of Overijssel and the Dutch Organization for Scientific Research NWO. We thank Theo van Oijen (XUV Optics) and Dennis IJpes (XUV Optics) for preparing the multilayer samples used in this work.

■ REFERENCES

(1) Takeyama, M.; Noya, A.; Fukuda, T. Thermal Stability of Cu/W/Si Contact Systems Using Layers of Cu(111) and W(110) Preferred Orientations. *J. Vac. Sci. Technol., A* **1997**, *15*, 415−420.

(2) Maniruzzaman, M.; Takeyama, M. B.; Hayasaka, Y.; Aoyagi, E.; Noya, A. Formation of Preferentially Oriented Cu [111] Layer on Nb [110] Barrier on SiO2. *Jpn. J. Appl. Phys., Part 2* **2004**, *43*, L1565−L1568.

(3) Zaytseva, I.; Abal'oshev, O.; Dłużewski, P.; Paszkowicz, W.; Zhu, L. Y.; Chien, C. L.; Kończykowski, M.; Cieplak, M. Z. Negative Hall Coefficient of Ultrathin Niobium in Si/Nb/Si Trilayers. *Phys. Rev. B: Condens. Matter Mater. Phys.* **2014**, *90*, 060505.

(4) Yusuf, S.; Iii, R. M. O.; Jiang, J. S.; Sowers, C. H.; Bader, S. D.; Fullerton, E. E.; Felcher, G. P. Magnetic profile in Nb/Si superconducting multilayers. *J. Magn. Magn. Mater.* **1999**, *198−199*, 564−566.

(5) Modi, M. H.; Rai, S. K.; Idir, M.; Schaefers, F.; Lodha, G. S. NbC/Si multilayer mirror for next generation EUV light sources. *Opt Express* **2012**, *20*, 15114.

(6) Ichimaru, S.; Ishino, M.; Nishikino, M.; Hatayama, M.; Hasegawa, N.; Kawachi, T.; Maruyama, T.; Inokuma, K.; Zenba, M.; Oku, S. Irradiation Damage Test of Mo/Si, Ru/Si and Nb/Si Multilayers Using the Soft X-Ray Laser Built at QST. In *X-Ray Lasers 2016*; Kawachi, T., Bulanov, S. V., Daido, H., Kato, Y., Eds.; Springer International Publishing: Cham, 2018, pp 303−308.

(7) Jang, S.-Y.; Lee, S.-M.; Baik, H.-K. Tantalum and Niobium as a Diffusion Barrier between Copper and Silicon. *J. Mater. Sci.: Mater. Electron.* **1996**, *7*, 1736−1738.

(8) Zhang, M.; Yu, W.; Wang, W. H.; Wang, W. K. Initial Phase Formation in Nb/Si Multilayers Deposited at Different Temperatures. *J. Appl. Phys.* **1996**, *80*, 1422−1427.

(9) Bochníček, Z.; Vávra, I. Interdiffusion in Amorphous Nb/Si Multilayers. *Mater. Lett.* **2000**, *45*, 120−124.

(10) Suresh, N.; Phase, D. M.; Gupta, A.; Chaudhari, S. M. Electron Density Fluctuations at Interfaces in Nb/Si Bilayer, Trilayer, and Multilayer Films: An x-Ray Reflectivity Study. *J. Appl. Phys.* **2000**, *87*, 7946−7958.

(11) Bochnícek, Z.; Vávra, I. Thermal Stability of Partially Crystalline Nb/Si Multilayers. *J. Phys. D: Appl. Phys.* **2001**, *34*, A214−A218.

(12) Okolo, B.; Lamparter, P.; Welzel, U.; Mittemeijer, E. J. Stress, Texture, and Microstructure in Niobium Thin Films Sputter Deposited onto Amorphous Substrates. *J. Appl. Phys.* **2004**, *95*, 466−476.

(13) Brongersma, H.; Draxler, M.; Deridder, M.; Bauer, P. Surface Composition Analysis by Low-Energy Ion Scattering. *Surf. Sci. Rep.* **2007**, *62*, 63−109.

(14) ter Veen, H. R. J.; Kim, T.; Wachs, I. E.; Brongersma, H. H. Applications of High Sensitivity-Low Energy Ion Scattering (HS-LEIS) in Heterogeneous Catalysis. *Catal. Today* **2009**, *140*, 197−201.

(15) Keim, E. G.; Bijker, M. D.; Lodder, J. C. Preparation of Cross-Sectional Transmission Electron Microscopy Specimens of Obliquely Deposited Magnetic Thin Films on a Flexible Tape. *J. Vac. Sci. Technol., A* **2001**, *19*, 1191−1194.

(16) Lisowski, W.; Keim, E. G.; Smithers, M. TEM and SEM Studies of Microstructural Transformations of Thin Iron Films during Annealing. *Appl. Surf. Sci.* **2002**, *189*, 148−156.

(17) Zameshin, A.; Makhotkin, I. A.; Yakunin, S. N.; van de Kruijs, R. W. E.; Yakshin, A. E.; Bijkerk, F. Reconstruction of Interfaces of Periodic Multilayers from X-Ray Reflectivity Using a Free-Form Approach. *J. Appl. Crystallogr.* **2016**, *49*, 1300−1307.

(18) Kessels, M. J. H.; Bijkerk, F.; Tichelaar, F. D.; Verhoeven, J. Determination of In-Depth Density Profiles of Multilayer Structures. *J. Appl. Phys.* **2005**, *97*, 093513.

(19) Sakhonenkov, S. S.; Filatova, E. O.; Gaisin, A. U.; Kasatikov, S. A.; Konashuk, A. S.; Pleshkov, R. S.; Chkhalo, N. I. Angle Resolved Photoelectron Spectroscopy as Applied to X-Ray Mirrors: An in Depth Study of Mo/Si Multilayer Systems. *Phys. Chem. Chem. Phys.* **2019**, *21*, 25002−25010.

(20) Sakhonenkov, S. S.; Filatova, E. O. Interface Formation between Be and W Layers Depending on Its Thickness and Ordering. *Appl. Surf. Sci.* **2020**, *534*, 147636.

(21) Coloma Ribera, R.; van de Kruijs, R. W. E.; Sturm, J. M.; Yakshin, A. E.; Bijkerk, F. In vacuo growth studies of Ru thin films on Si, SiN, and SiO2 by high-sensitivity low energy ion scattering. *J. Appl. Phys.* **2016**, *120*, 065303.

(22) Chandrasekaran, A.; van de Kruijs, R. W. E.; Sturm, J. M.; Zameshin, A. A.; Bijkerk, F. Nanoscale Transition Metal Thin Films: Growth Characteristics and Scaling Law for Interlayer Formation. *ACS Appl. Mater. Interfaces* **2019**, *11*, 46311−46326.

(23) Zameshin, A. Probing atmoic scale interface processes using X-rays and ions. *Probing Atmoic Scale Interface Processes Using X-Rays and Ions*; University of Twente: Enschede, The Netherlands, 2018.

(24) Brüner, P.; Grehl, T.; Brongersma, H.; Detlefs, B.; Nolot, E.; Grampeix, H.; Steinbauer, E.; Bauer, P. Thin Film Analysis by Low-Energy Ion Scattering by Use of TRBS Simulations. *J. Vac. Sci. Technol., A* **2015**, *33*, 01A122.

(25) Alford, T. L.; Feldman, L. C. Ion Channeling. *Fundamentals of Nanoscale Film Analysis*; Springer US: Boston, MA, 2007; pp 84−104.

(26) Shutthanandan, V.; Zhu, Z.; Stutzman, M. L.; Hannon, F. E.; Hernandez-Garcia, C.; Nandasiri, M. I.; Kuchibhatla, S. V. N. T.; Thevuthasan, S.; Hess, W. P. Surface Science Analysis of GaAs Photocathodes Following Sustained Electron Beam Delivery. *Phys. Rev. Spec. Top.–Accel. Beams* **2012**, *15*, 063501.

(27) Bajt, S.; Stearns, D. G.; Kearney, P. A. Investigation of the Amorphous-to-Crystalline Transition in Mo/Si Multilayers. *J. Appl. Phys.* **2001**, *90*, 1017−1025.

(28) Vitos, L.; Ruban, A. V.; Skriver, H. L.; Kollár, J. The Surface Energy of Metals. *Surf. Sci.* **1998**, *411*, 186−202.

(29) Eberl, C.; Liese, T.; Schlenkrich, F.; Döring, F.; Hofsäss, H.; Krebs, H.-U. Enhanced resputtering and asymmetric interface mixing in W/Si multilayers. *Appl. Phys. A: Mater. Sci. Process.* **2013**, *111*, 431−437.

(30) Gupta, A.; Kumar, D.; Phatak, V. Asymmetric Diffusion at the Interfaces in Fe/Si Multilayers. *Phys. Rev. B: Condens. Matter Mater. Phys.* **2010**, *81*, 1−5.

(31) Li, H.; Zhu, J.; Wang, Z.; Song, Z.; Chen, H. Asymmetrical Diffusion at Interfaces of Mg/SiC Multilayers. *Opt. Mater. Express* **2013**, *3*, 546.

(32) de Boer, F. R.; Boom, R.; Mattens, W. C. M.; Miedema, A. R.; Niessen, A. K. *Cohesion in Metals: Transition Metal Alloys*, 1988.

(33) McKeown, J. T.; Radmilovic, V. R.; Gronsky, R.; Glaeser, A. M. Silicide Characterization at Alumina-Niobium Interfaces. *J. Mater. Sci.* **2011**, *46*, 3969−3981.
(34) Cahn, R. W. Binary Alloy Phase Diagrams-Second Edition. T. B. Massalski, Editor-in-Chief; H. Okamoto, P. R. Subramanian, L. Kacprzak, Editors. ASM International, Materials Park, Ohio, USA. December 1990. Xxii, 3589 Pp., 3 Vol., Hard- Back. $995.00 the Set. *Adv. Mater.* **1991**, *3*, 628−629.
(35) Bruijn, S.; Van De Kruijs, R. W. E.; Yakshin, A. E.; Bijkerk, F. In-Situ Study of the Diffusion-Reaction Mechanism in Mo/Si Multilayered Films. *Appl. Surf. Sci.* **2011**, *257*, 2707−2711.
(36) Huang, Q.; Zhang, J.; Qi, R.; Yang, Y.; Wang, F.; Zhu, J.; Zhang, Z.; Wang, Z. Structure and stress studies of low temperature annealed W/Si multilayers for the X-ray telescope. *Express* **2016**, *24*, 15620.

https://doi.org/10.1021/acsami.1c06210
ACS Appl. Mater. Interfaces 2021, 13, 31260−31270